

Deep Charging Characteristics of Dielectric-Conductor Alternating Structures Under High-Energy Electron Irradiation (Postprint)

Authors: Zheng Hansheng, Yang Tao, Han Jianwei, Zhang Zhenlong, Liu Jikui

Date: 2017-03-10T00:00:00+00:00

Abstract

Dielectric-conductor alternating structures are common configurations in spacecraft components. To investigate the intrinsic factors affecting the deep charging characteristics of such structures, experimental samples with different configurations were designed, and deep charging irradiation experiments were conducted on the samples using an Sr-90 radioactive source to simulate the space high-energy electron environment, with the differences in charging potential measured. Additionally, with the aid of three-dimensional deep charging simulation software, the deep charging potential and electric field distribution of such structures under different geometric configurations were calculated. Experimental and simulation results demonstrate that both the maximum dielectric surface potential and the maximum electric field inside the dielectric are positively correlated with the dielectric width and height. When other conditions remain unchanged, the wider the dielectric or the higher it is above the conductor surface, the greater the risk of discharge. In cases where tiny gaps exist between the dielectric and conductor sidewalls, the maximum electric field inside the dielectric is significantly enhanced, making internal breakdown more likely to occur. Moreover, in the vacuum gap between the dielectric and conductor, the electric field can easily exceed the breakdown threshold, posing a significant discharge risk under certain triggering conditions. In aerospace engineering applications, to reduce the risk of deep charging and discharging in such structures, the dielectric width should be minimized, the height difference between the dielectric and conductor should be reduced, and good sidewall contact between the dielectric and conductor should be ensured, provided that insulation performance and other requirements are satisfied.

Full Text

Study on Deep Dielectric Charging Characteristics of Dielectric-Conductor Adjacent Structures under Energetic Electron Irradiation

ZHENG Han-sheng^{1,2}, YANG Tao¹, HAN Jian-wei^{1,2}, ZHANG Zhen-long^{1,2}, LIU Ji-kui³ ¹. National Space Science Center, Chinese Academy of Sciences, Beijing 100190, China

². University of Chinese Academy of Sciences, Beijing 100049, China

³. Beijing Institute of Control Engineering, Beijing 100190, China

Abstract

Dielectric-conductor adjacent structures are common in spacecraft components. To investigate the intrinsic factors influencing the deep dielectric charging characteristics of such structures, experimental samples with different configurations were designed and irradiated using an Sr-90 source to simulate the energetic electron environment in space, with charging potential differences measured during the experiments. Additionally, a three-dimensional deep charging simulation software was employed to numerically calculate the deep charging potential and electric field distributions for these structures under various geometric configurations. Both experimental and simulation results demonstrate that the maximum dielectric surface potential and internal electric field correlate positively with the dielectric width and height (relative to the conductor surface). Under otherwise identical conditions, wider dielectrics or those extending further above the conductor surface exhibit higher discharge risk. Particularly when a minute gap exists between the dielectric and conductor sidewalls, the maximum electric field inside the dielectric intensifies significantly, predisposing the structure to internal breakdown. Moreover, the electric field within the vacuum gap between dielectric and conductor can readily exceed the breakdown threshold, creating substantial discharge risk under certain triggering conditions. For aerospace engineering applications, to mitigate deep charging and discharging risks in such structures, dielectric width and height differential should be minimized while ensuring adequate insulation performance, and good sidewall contact between dielectric and conductor must be guaranteed.

Keywords: energetic electron; deep dielectric charging; experiment; three-dimensional simulation

In the space radiation environment, high-energy electrons possess strong penetration capability and readily deposit within insulating dielectrics on spacecraft exteriors or penetrate shielding layers to deposit in internal dielectrics and on isolated conductor surfaces. This sustained charge accumulation leads to deep dielectric charging (also termed internal charging) effects, with resulting electrostatic discharges representing a primary space environmental hazard [1-3]. The

hazard becomes particularly pronounced in the harsh electron environment of Earth's outer radiation belt, where energetic electron fluxes (hundreds of keV to several MeV) can increase by 2-3 orders of magnitude within days during regular or sporadic high-energy electron storms [4,5], seriously threatening the safe and reliable operation of geostationary orbit (GEO), medium Earth orbit (MEO), and highly elliptical orbit (HEO) satellites [6-8].

Deep dielectric charging research primarily focuses on high-resistivity dielectric materials commonly used in aerospace applications. Isolated conductors that are not properly grounded should be strictly avoided. Structures containing large dielectric volumes, such as cable jackets, circuit boards, and various insulating supports and fasteners, constitute high-risk locations for deep charging. While numerous studies have investigated deep charging simulation experiments and computational modeling for simple configurations like planar dielectrics [9-11], relatively few have examined the charging characteristics of more complex representative satellite configurations [12,13]. In reality, on-orbit charging and discharging constitute complex physical processes dependent not only on material properties but also on specific structural configurations, grounding conditions, and surrounding layouts. Simplifying these structures to one-dimensional planar models is often inappropriate. Therefore, investigating the charging characteristics and behavior of typical satellite component structures with high deep charging risk through experimental and simulation approaches holds significant importance for deep charging protection design in aerospace engineering applications.

A dielectric-conductor adjacent structure refers to a configuration where dielectric and conductor materials are in direct lateral contact, with the conductor providing a sidewall grounding path for the dielectric. This structure commonly appears in the conductive ring assemblies of Solar Array Drive Assemblies (SADA). Solar panels transmit power and signals to the spacecraft bus through metal slip rings and brushes in the SADA conductive ring, with insulating dielectrics separating different metal slip rings [14]. Since SADA is installed at the interface between the spacecraft body and outer space, high-energy electrons can penetrate the SADA housing, causing severe deep charging effects in the insulating dielectrics between conductive slip rings. Should dielectric charging induce discharge to a conductive slip ring, the discharge pulse may affect solar panel tracking control and reliable spacecraft power supply. This study employs an Sr-90 source to simulate the high-energy electron environment of the outer radiation belt, designs experimental samples of dielectric-conductor adjacent structures with various configurations, conducts deep charging irradiation experiments, and utilizes an independently developed three-dimensional internal charging simulation software to calculate charging potential and electric field distributions for different dielectric widths, heights, and gap conditions, thereby analyzing the various intrinsic factors influencing the deep charging characteristics of dielectric-conductor adjacent structures.

1.1 Experimental Apparatus

The Spacecraft Charging and Discharging Simulator (SCADS) at the National Space Science Center, Chinese Academy of Sciences, is a dedicated experimental facility for investigating spacecraft material charging-discharging characteristics and assessing charging risks for satellite components and equipment [15], as shown in [FIGURE:1]. The apparatus consists primarily of a vacuum chamber with pumping system, electron irradiation sources, temperature-controlled sample stage, shielding and transmission system, and parameter measurement system. Its core components are two distinct electron irradiation sources: a STAIB EK-100-FL electron gun and an array of seven Sr-90/Y-90 radioactive sources with a total activity of 350 mCi. The electron gun provides a monoenergetic electron beam with continuously adjustable current density in the 5-100 keV energy range, while the Sr-90/Y-90 sources emit electrons with a continuous energy spectrum ($E_{\text{max}} = 2.28$ MeV) through β decay at flux levels around $\mu\text{A}/\text{cm}^2$, providing good matching with the energy spectrum and flux of deep charging electrons in the outer radiation belt and serving as an ideal deep charging simulation source. To simulate various levels of harsh high-energy electron environments, the electron flux can be controlled by adjusting the distance between the radioactive source and experimental samples. During irradiation experiments, the parameter measurement system automatically monitors and records charging-discharging parameters including sample surface potential, ground current, discharge current pulses, electric field pulses, and discharge images.

1.2 Experimental Samples

To comparatively investigate the effects of dielectric width and height (the height difference between dielectric and conductor surfaces) on deep charging behavior in dielectric-conductor adjacent structures, two experimental samples (#1 and #2) were designed with the cross-sectional structures shown in

. Both samples measure $98 \text{ mm} \times 60 \text{ mm} \times 8 \text{ mm}$, with polyimide dielectric and copper conductor materials. Copper strips 2 mm thick are embedded in insulating grooves of different depths (6 mm and 4 mm). In sample #1, both the copper strips and the dielectric sections between them have a width of 10 mm, while in sample #2, both have a width of 5 mm.

The conductor in lateral contact with the dielectric (non-isolated) provides a charge dissipation path for deposited charges within the dielectric. Should poor contact create minute gaps between conductor and dielectric, charge dissipation would be adversely affected. To investigate charging effects under such conditions, sample #3 was designed with dimensions of $40 \text{ mm} \times 40 \text{ mm} \times 8 \text{ mm}$, using polytetrafluoroethylene (PTFE) dielectric and copper conductor materials, as shown in

. The copper strip is 2 mm thick with a 4 mm height difference between dielectric and copper surfaces, with one copper strip having a 0.1 mm gap between its

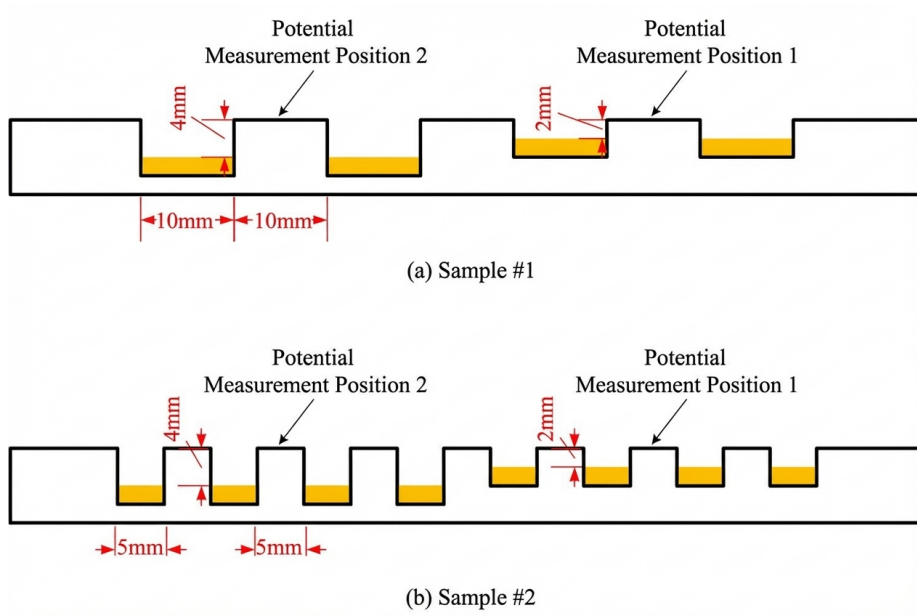


Figure 1: Figure 2

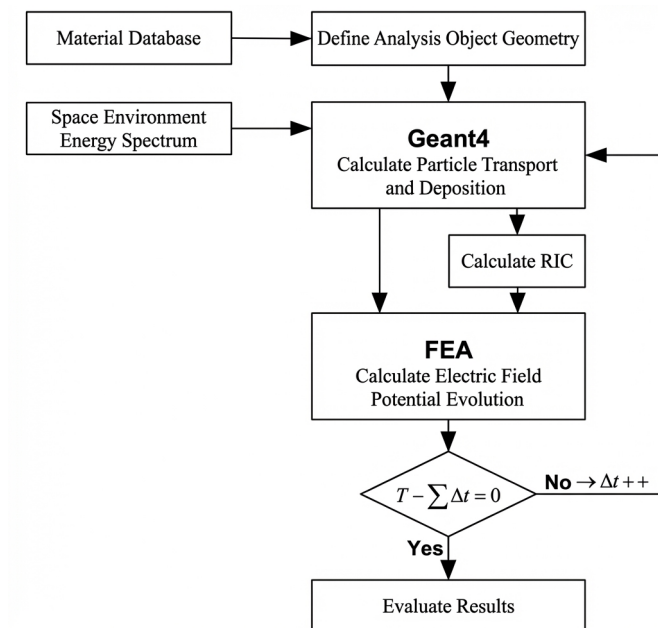


Figure 2: Figure 3

sidewall and the dielectric.

Considering that in engineering applications the voltage applied to SADA conductive ring slip rings is negligible compared to dielectric charging voltage, all copper strips in the experimental samples were grounded. During experiments, the front surface (the grooved side) received electron irradiation. The radioactive source was positioned directly in front of the sample, with source distance adjusted to achieve an electron flux of 5 pA/cm^2 at the sample center. Throughout the experiments, vacuum pressure was maintained at 10^{-10} Pa and temperature was kept at room temperature. Surface potentials at two symmetric positions on each sample were measured non-contactly to compare charging potential differences.

1.3 Simulation Software and Modeling

While simulation experiments can obtain key charging-discharging parameters such as surface potential and discharge current pulses, they lack effective measurement means for internal dose deposition details and electric field/potential distributions. Computer simulation can compensate for these experimental limitations by flexibly selecting input spectrum parameters, calculating dose deposition distributions, and providing temporal and spatial evolution of charging potential and internal electric fields.

SIC3D is a three-dimensional deep charging simulation software independently developed at the National Space Science Center, capable of geometric modeling and simulation calculations for satellite components with complex three-dimensional structures [16,17]. Its basic framework is shown in [FIGURE:4]. The deep charging calculation involves two fundamental physical processes: transport of space radiation electrons within dielectric materials and evolution of built-in electric fields within dielectrics. Correspondingly, SIC3D comprises two main modules: a Geant4-based Monte Carlo electron transport module for calculating high-energy electron trajectories and energy deposition in materials, and a Finite Element Analysis (FEA)-based electric field evolution module that solves the charge continuity equation incorporating the Radiation-Induced Conductivity (RIC) model and Poisson's equation to compute the evolution of built-in electric fields.

Using SIC3D, geometric modeling and charging simulations were performed for dielectric-conductor adjacent structures. As shown in [FIGURE:5], four different three-dimensional models were established with varying dielectric widths, heights, and minute gaps between dielectric and conductor. All four models use polyimide (PI) dielectric material and 2 mm thick copper strips. In model (a), the dielectric adjacent to copper strips is 10 mm wide and 2 mm high; model (b) has 10 mm wide and 4 mm high dielectric; model (c) has 5 mm wide and 2 mm high dielectric; model (d) has the same dielectric width and height as model (a) but includes a 0.1 mm gap between copper strip and dielectric. Dielectric material parameters used in calculations are listed in , with copper strips set at zero

potential. To facilitate qualitative comparison with experimental results, the simulation electron source employed the Sr-90 source spectrum, incident from above the model with electron flux consistent with experiments (5 pA/cm^2).

2.1 Influence of Dielectric Width and Height on Deep Charging Characteristics

Under Sr-90 source irradiation, the potential evolution at the two measurement positions for samples #1 and #2 is shown in [FIGURE:6]. After approximately 2000 minutes, surface potentials approached equilibrium. Sample #1 reached equilibrium potentials of about $-14,000 \text{ V}$ at position 1 and $-16,500 \text{ V}$ at position 2, while sample #2 reached $-13,000 \text{ V}$ at position 1 and $-15,000 \text{ V}$ at position 2. The surface potentials at both measurement positions on sample #1 exceeded those at corresponding positions on sample #2, indicating that for identical dielectric-conductor height differences, wider dielectrics develop higher charging potentials. Furthermore, for both samples, potentials at position 2 exceeded those at position 1, demonstrating that increased dielectric-conductor height difference elevates charging potential.

Three-dimensional distributions of charging potential and internal electric field for models (a), (b), and (c) calculated using SIC3D are shown in [FIGURE:7] and

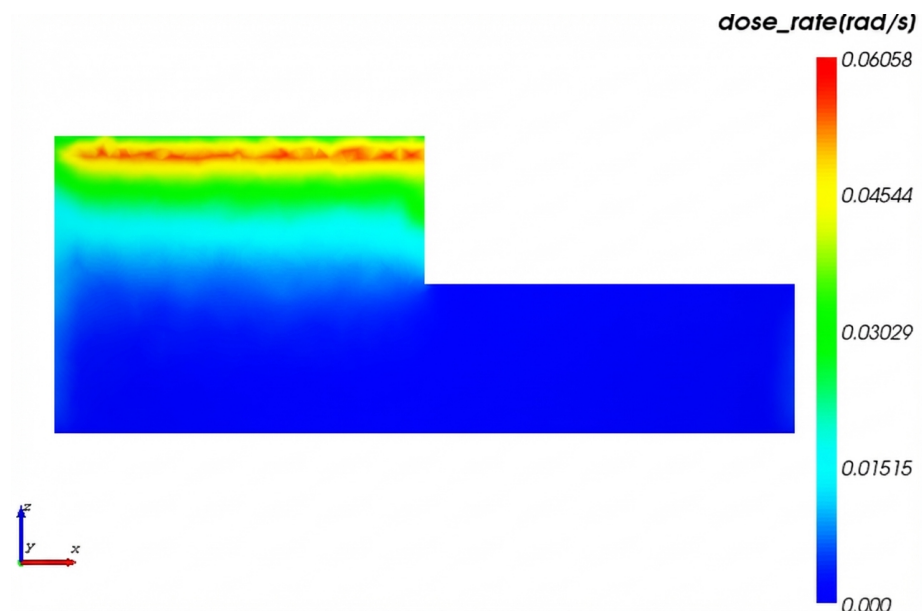


Figure 3: Figure 8

. The distributions exhibit similar patterns across different dielectric widths and heights. The highest negative surface potential appears at the location

farthest from the copper strip (ground point). If dielectrics are adjacent to grounded conductors on both sides, the maximum negative potential would occur at the dielectric center. The maximum internal electric field appears at the interface between dielectric sidewall and grounded copper strip, similar to deep charging calculation results for planar dielectrics grounded on front, back, or both surfaces [10].

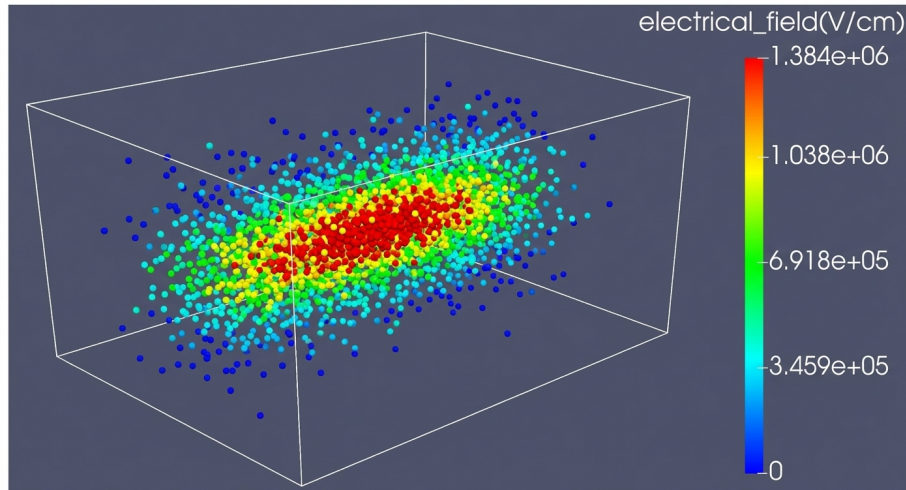


Figure 4: Figure 9

shows the variation of maximum dielectric surface potential and internal electric field with dielectric width and height obtained through SIC3D simulation. Whether internal breakdown discharge occurs depends on whether the maximum internal electric field exceeds the material's dielectric strength. The variation of maximum electric field with width and height reveals that the built-in electric field from deep charging intensifies as dielectric width or height increases. The enhancement of maximum electric field with increasing width relates to the enlarged electron irradiation area. Assuming electron incident flux J_I , dielectric irradiation area S_I , ground area S_O , built-in electric field near the ground plane E , and conductivity σ , charge conservation and Ohm's law at charging equilibrium yield:

$$\iint \mathbf{J} \cdot d\mathbf{S} = \iint \sigma \mathbf{E} \cdot d\mathbf{S}$$

With other conditions constant, increasing dielectric width enlarges the exposed irradiation area S_I , resulting in stronger local electric fields near the dielectric ground plane and increased internal breakdown risk.

The effect of dielectric height on maximum electric field relates to the dose rate distribution at different depths.

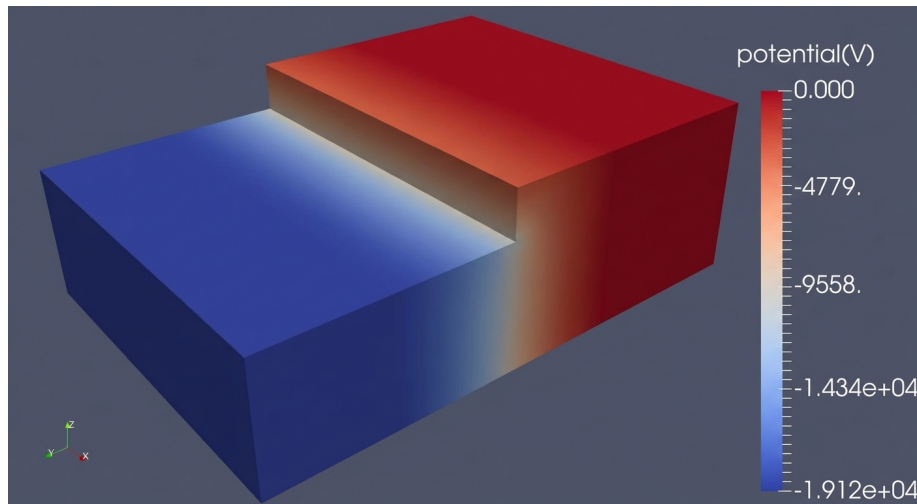


Figure 5: Figure 10

shows the dose rate distribution in the $y=0$ plane of model (a) calculated via Monte Carlo methods. The right half of the dielectric receives no electron penetration due to shielding by the 2 mm thick copper strip. In the left half, dose rate decreases along the vertical direction from the dielectric surface. Limited by the maximum range of incident electrons in polyimide, dose rate becomes nearly zero below approximately 4 mm from the surface. The conductivity of dielectric under radiation is:

$$\sigma = \sigma_{\text{dark}} + \sigma_{\text{RIC}} = \sigma_{\text{dark}} + k_p \dot{D}^\Delta$$

When the dose rate is 0.01 rad/s and using material parameters from , the radiation-induced conductivity of polyimide exceeds its dark conductivity by an order of magnitude. Therefore, when the dielectric-conductor surface height difference exceeds the maximum electron range, the drastically reduced conductivity near the ground plane (σ_{dark}) significantly enhances the maximum internal electric field according to Ohm' s law $J = E$.

From the charging potential simulation results, surface potential, like maximum electric field, correlates positively with dielectric width and height under certain conditions. Potential being the spatial integral of electric field, surface potential depends on internal field strength and distance to ground points. Among models (a), (b), and (c), model (b) exhibits both stronger internal electric fields and greater distance from the dielectric top edge to ground points, resulting in higher surface potential. Surface potential not only indirectly reflects internal field magnitude but more directly influences discharge risk between the dielectric surface and nearby component surfaces. If the potential difference be-

tween adjacent surfaces produces interfacial electric fields exceeding breakdown thresholds, discharge will occur. Therefore, in dielectric-conductor adjacent structures, to reduce risks of both internal breakdown discharge and surface-to-surface discharge, dielectric width and height differential should be minimized while meeting other requirements.

2.2 Influence of Dielectric-Conductor Gap on Deep Charging Characteristics

Sample #3 was irradiated with the Sr-90 source for over 24 hours to reach charging equilibrium, with no discharge pulses detected during irradiation. [FIGURE:11] shows the potential evolution at two measurement positions. Significant differences appear between positions 1 and 2 surface potentials. At position 1, where dielectric-copper contact was good, equilibrium surface potential reached approximately -6,100 V. At position 2, where a 0.1 mm gap existed between dielectric sidewall and copper strip, surface potential was 32.8% higher at -8,100 V.

Three-dimensional charging simulation results for model (d) are shown in [FIGURE:12]. With a gap present, the maximum dielectric surface potential reaches -19,000 V, an order of magnitude higher than the -9,146 V maximum potential in model (a). Comparing electric field calculations between models (a) and (d) reveals even more significant differences in maximum electric field magnitude and distribution details. Without a gap, the maximum electric field is 7.4×10 V/cm, located within the dielectric at the copper strip sidewall interface. With a gap, the overall maximum electric field occurs in the upper vacuum gap region between dielectric and conductor sidewalls, reaching 1.4×10 V/cm, while the maximum electric field within the dielectric occurs near the copper strip edge at the gap bottom, approximately 3.5×10 V/cm. Both values exceed threshold electric field criteria for possible vacuum gap discharge and dielectric breakdown discharge given in NASA-HDBK-4002A [18], with the gap region field strength exceeding breakdown threshold by an order of magnitude.

The dramatic enhancement of charging potential and electric field due to dielectric-conductor gaps results from altered charge dissipation pathways. With good sidewall contact, charges within the dielectric dissipate primarily through the conductor sidewall over a large area and short distance. When poor contact creates minute gaps, charges must detour to the contact point at the gap bottom (the conductor bottom edge). Since the dielectric beneath this location receives no electron irradiation due to copper shielding, only dark conductivity participates in charge dissipation, causing significant local electric field enhancement. In the vacuum gap between dielectric and conductor, the combination of large potential difference across the gap and extremely small gap dimensions can produce electric fields exceeding breakdown thresholds, creating high discharge risk under triggering conditions (e.g., dielectric outgassing). Therefore, ensuring good electrical contact between dielectric and conductor sidewalls is critically important in engineering applications.

3 Summary

This study conducted deep charging irradiation experiments on dielectric-conductor adjacent structure samples with various configurations using the Sr-90 source of the Spacecraft Charging and Discharging Simulator, and calculated potential and electric field distributions at charging equilibrium for different geometric models using the three-dimensional deep charging simulation software SIC3D. Experimental and simulation results demonstrate that under continuous-spectrum high-energy electron irradiation, both the maximum surface potential of dielectrics adjacent to conductors and the maximum internal electric field correlate positively with dielectric width and height. Under otherwise constant conditions, wider dielectrics or those extending further above the conductor surface exhibit higher discharge risk between adjacent components and greater internal breakdown risk. Particularly when minute gaps arise from poor contact between dielectric and conductor sidewalls, altered charge dissipation pathways cause dramatic enhancement of the maximum internal electric field, increasing field strength by an order of magnitude. In the narrow vacuum region of such gaps, electric fields readily exceed breakdown thresholds, enabling dielectric-conductor discharge when gap dimensions are small. For dielectric-conductor adjacent structures in spacecraft (e.g., SADA conductive rings), dielectric width and height differential should be minimized while ensuring adequate inter-conductor insulation performance, and good electrical contact between dielectric and conductor sidewalls must be guaranteed to eliminate gap formation.

References

- [1] Frederickson A R. Upsets related to spacecraft charging[J]. IEEE Transactions on Nuclear Science, 1996, 43(2): 426-441.
- [2] Griseri V. Behavior of dielectrics in a charging space environment and related anomalies in Flight[J]. IEEE Transactions on Dielectrics and Electrical Insulation, 2009, 16(3): 689-695.
- [3] Quan Ronghui. Characteristics and Effects of Spacecraft Deep Dielectric Charging[D]. PhD Dissertation. Beijing: University of Chinese Academy of Sciences, 2010.
- [4] Pu Zuyin, Yu Bin, Xie Lun, et al. Magnetosphere energetic electron storm[J]. Science in China (Series A), 2000, 30(Suppl): 127-130.
- [5] Yan Xiaojuan, Chen Dong, Huang Jianguo, et al. A space energetic electron environment model for spacecraft deep dielectric charging evaluation[J]. Spacecraft Environment Engineering, 2008, 25(2): 120-124.
- [6] Han Jianwei, Huang Jianguo, Liu Zhenxing, et al. Correlation of double star anomalies with space environment[J]. Journal of Spacecraft and Rockets, 2005, 42(6): 1061-1065.

- [7] Huang Jianguo, Han Jianwei. Analysis of a typical internal charging induced spacecraft anomaly[J]. *Acta Physica Sinica*, 2010, 59(4): 2907-2913.
- [8] Ecoffet R. Overview of in-orbit radiation induced spacecraft anomalies[J]. *IEEE Transactions on Nuclear Science*, 2013, 60(3): 1791-1815.
- [9] Jun I, Garrett H B, Kin W, et al. Review of an internal charging code, NUMIT[J]. *IEEE Transactions on Nuclear Science*, 2008, 36(5): 2467-2472.
- [10] Huang Jianguo, Chen Dong. A study of deep dielectric charging on satellites by computer simulation[J]. *Chinese Journal of Geophysics*, 2004, 47(3): 392-397.
- [11] Tang Xiaojin, Yi Zhong, Zhang Chao, et al. Study on computation of build-up electric field in FR-4 circuit board for satellite[J]. *Equipment Environmental Engineering*, 2009, 6(4): 33-38.
- [12] Zhang Zhenlong, Qun Ronghui, Han Jianwei, et al. Internal charging-discharging test and simulation for satellite components[J]. *Atomic Energy Science and Technology*, 2010, 44(Suppl): 538-544.
- [13] Yi Zhong, Wang Song, Tang Xiaojin, et al. Computer simulation on temperature-dependent internal charging of complex dielectric structure[J]. *Acta Physica Sinica*, 2015, 64(12): 125201-125201.
- [14] Li Rui, Liu Jikui, Xu Yuemin, et al. Study of surface charging and discharging effects on solar array drive assembly[J]. *Chinese Journal of Space Science*, 2014, 34(3): 360-366.
- [15] Zhang Zhenlong, Quan Ronghui, Wang Yan, Han Jianwei. Ground testing and computer modeling of internal charging for complex structures[C]. *The 12th Spacecraft Charging Technology Conference*, Kitakyushu, Japan, May 14-18, 2012.
- [16] Sun Jianjun, Zhang Zhenlong, Liang Wei, et al. Simulation of internal charging for electric cables used in the satellite[J]. *Spacecraft Environment Engineering*, 2014, 31(2): 173-177.
- [17] Zhang Zhenlong, Zhu Lihua, Han Jianwei, Gong Ding. A three-dimensional tool for spacecraft internal charging[C]. *AIAA Space and Astronautics Forum and Exposition 2015*, Pasadena, USA, August 29-September 2, 2015.
- [18] Michael G R. Mitigating In-Space Charging Effects—A Guideline[R]. *NASA-HDBK-4002A*, 2011.

Author Biographies:

ZHENG Han-sheng (1989—), male, PhD candidate, research focus: space environmental effects; Correspondence address: No. 1 Zhongguancun South Second Street, Haidian District, Beijing; Phone: 13161079232; E-mail: zhenghansheng12@mails.ucas.ac.cn

HAN Jian-wei (1970—), male, PhD, professor, research focus: space environmental effects; Correspondence address: P.O. Box 8701, Beijing 100190; Phone:

(010)62582852; E-mail: hanjw@nssc.ac.cn

Source: ChinaXiv – Machine translation. Verify with original.